

Ectopic *Meis1* expression in the mouse limb bud alters P-D patterning in a *Pbx1*-independent manner

NADIA MERCADER¹, LICIA SELLER², LUIS MIGUEL CRIADO¹, PILAR PALLARES¹, CARLOS PARRAS³,
MICHAEL L. CLEARY⁴ and MIGUEL TORRES^{*,1}

¹Centro Nacional de Investigaciones Cardiovasculares (CNIC), Instituto de Salud Carlos III, Madrid, Spain,

²Department of Cell and Developmental Biology, Cornell University Weill Medical School, New York, USA,

³INSERM U711, Université Pierre et Marie Curie, IFR de Neurosciences, Hôpital de la Salpêtrière, Paris, France and

⁴Department of Pathology, Stanford University School of Medicine, Stanford, USA

ABSTRACT During limb development, expression of the TALE homeobox transcription factor *Meis1* is activated by retinoic acid in the proximal-most limb bud regions, which give rise to the upper forelimb and hindlimb. Early subdivision of the limb bud into proximal *Meis*-positive and distal *Meis*-negative domains is necessary for correct proximo-distal (P-D) limb development in the chick, since ectopic *Meis1* overexpression abolishes distal limb structures, produces a proximal shift of limb identities along the P-D axis, and proximalizes distal limb cell affinity properties. To determine whether *Meis* activity is also required for P-D limb specification in mammals, we generated transgenic mice ectopically expressing *Meis1* in the distal limb mesenchyme under the control of the *Msx2* promoter. *Msx2:Meis1* transgenic mice display altered P-D patterning and shifted P-D *Hox* gene expression domains, similar to those previously described for the chicken. *Meis* proteins function in cooperation with PBX factors, another TALE homeodomain subfamily. *Meis*-*Pbx* interaction is required for nuclear localization of both proteins in cell culture, and is important for their DNA-binding and transactivation efficiency. During limb development, *Pbx1* nuclear expression correlates with the *Meis* expression domain, and *Pbx1* has been proposed as the main *Meis* partner in this context; however, we found that *Pbx1* deficiency did not modify the limb phenotype of *Msx2:Meis1* mice. Our results indicate a conserved role of *Meis* activity in P-D specification of the tetrapod limb and suggest that *Pbx* function in this context is either not required or is provided by partners other than *Pbx1*.

KEY WORDS: mouse limb development, proximo-distal axis, *Meis1*, *Pbx*

Introduction

The vertebrate limb is an excellent model in which to study the genetic control of developmental processes (Capdevila and Izpisua Belmonte, 2001, Tickle, 2002). The mesoderm-ectoderm interactions, cell migrations and patterning events that take place during limb formation involve signaling molecules and transcription factors that also operate during the development of other structures and organs. Learning about the gene regulatory network involved in limb outgrowth will therefore provide valuable insights into developmental processes occurring elsewhere. The limb bud arises from a subset of undifferentiated lateral plate mesoderm (LPM) cells covered by an ectodermal cap, and forms a lateral protrusion from the main anterior-posterior axis of the embryo.

During subsequent growth, cells within the limb bud acquire positional information and translate it into specific patterns of differentiated tissues across the three main limb axes. Along the limb proximo-distal (P-D) axis three main segments are generated: the stylopod (upper arm/leg), zeugopod (lower arm/leg) and autopod (hand- and footplate). These elements arise sequentially during limb outgrowth: elements closer to the trunk (proximal) form first, and the tips of the digits, which lie at the distal-most end of the limb, are the last cartilage element to differentiate (Saunders, 1948, Summerbell *et al.*, 1973).

In the past decade, molecular markers have been character-

Abbreviations used in this paper: AER, apical ectodermal ridge; P-D, proximo-distal.

***Address correspondence to:** Miguel Torres. Centro Nacional de Investigaciones Cardiovasculares, Melchor Fernández Almagro, 3, 28029 Madrid, Spain.
Fax: +34-91-453-1304. e-mail: mtorres@cnic.es

Final author-corrected PDF published online: 19th May 2008.

ISSN: Online 1696-3547, Print 0214-6282

© 2008 UBC Press
Printed in Spain

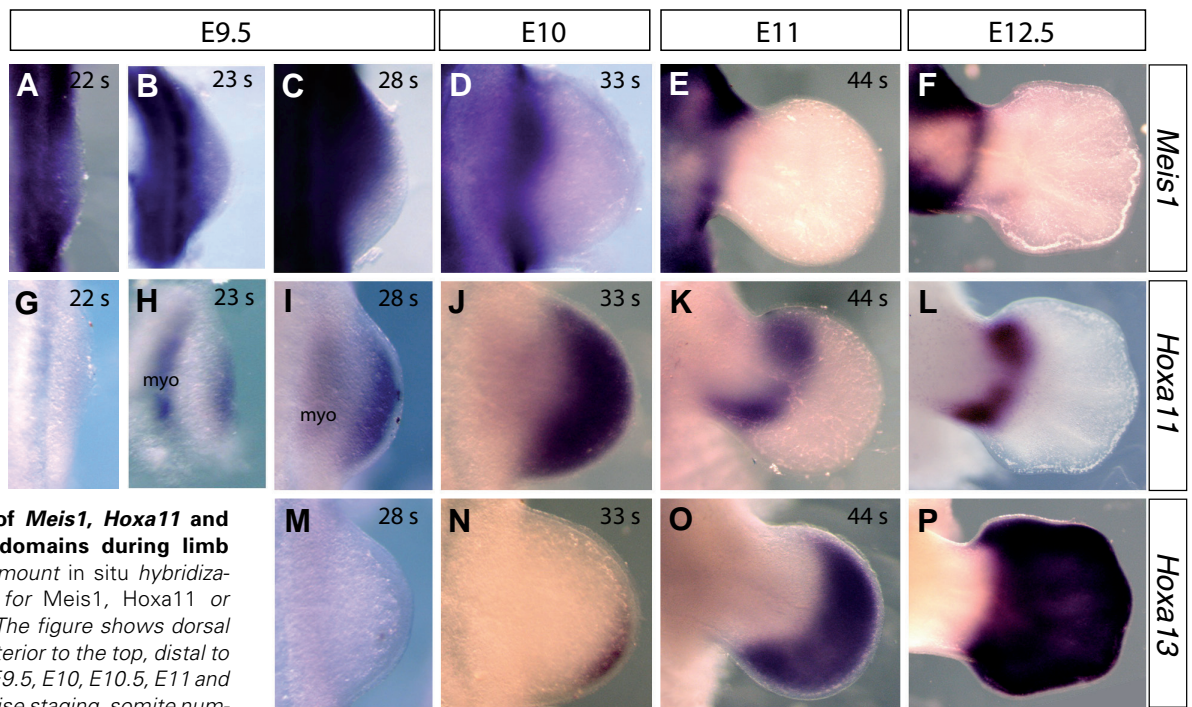


Fig. 1. Comparison of *Meis1*, *Hoxa11* and *Hoxa13* expression domains during limb development. Wholemount in situ hybridization with riboprobes for *Meis1*, *Hoxa11* or *Hoxa13* as indicated. The figure shows dorsal views of forelimbs (anterior to the top, distal to the right) from stages E9.5, E10, E10.5, E11 and E12.5. For a more precise staging, somite number (s) was counted for the younger embryos.

(A/G), (B/H), (J/N) and (E/K) are forelimbs from the same embryos, with the images in (G,H,N,E) inverted to enable better comparison of the expression patterns. myo indicates the somite-derived *Hoxa11*-positive myoblast population migrating into the limb bud.

ized that define the precursor regions of the main P-D segments in the early limb bud. The *Hox* genes *Hoxa11* and *Hoxa13* are expressed in the zeugopod and autopod, respectively (Yokouchi, *et al.*, 1991). In the chick, overexpression of *Hoxa13* leads to defects in zeugopod cartilage formation and altered cell adhesiveness; the resulting phenotype resembles a change of cell fate towards autopodal cartilage, forming shorter elements than those of the wildtype radius and ulna from the zeugopod (Yokouchi *et al.*, 1995). During development, *Hoxa11* and *Hoxa13* expression domains partially overlap with those of their *Hoxd* cluster orthologs (Dollé *et al.*, 1989; Nelson *et al.*, 1996). Double mutants for *Hoxa13* and *Hoxd13* reveal defects in autopod cartilage formation that suggest additive functions for these two genes (Fromental-Ramain *et al.*, 1996). Similarly, analysis of *Hoxa11/Hoxd11* double mutant limbs has revealed additive functions for this gene pair during zeugopod development (Davis *et al.*, 1995). These data suggest that Hox function within each P-D segment is achieved by the additive effects of two or more orthologous genes belonging to different Hox clusters. While *Hoxa11* and *Hoxa13* are the best markers available for zeugopod and autopod, their loss-of-function phenotypes do not support a role in specifying segmental identity in the limb, but rather in determining growth rates and adequate differentiation schedules for each segment (Boulet and Capecchi, 2004).

The expression patterns of members of another homeobox transcription factor (TF) family, the TALE homeobox TFs *Meis1* and *Meis2* (Moskow *et al.*, 1995; Nakamura *et al.*, 1996), define the proximal-most segments of the limb, including the stylopod and more proximal regions. *Meis1* and *Meis2* are expressed in the embryonic LPM (Cecconi *et al.*, 1997; Mercader *et al.*, 1999; Oulad-Abdelghani *et al.*, 1997). During limb outgrowth, their

expression becomes restricted to a proximal region of the limb bud mesenchyme and ectoderm. When overexpressed throughout the chick limb bud, *Meis1* and *2* each induce alterations in zeugopod and autopod formation (Capdevila *et al.*, 1999; Mercader *et al.*, 1999). The defects observed range from proximalization of the P-D limb axis (Mercader *et al.*, 1999) to deletion of distal segments (Capdevila *et al.*, 1999; Mercader *et al.*, 1999). P-D limb axis proximalization in these studies was evident from the altered distributions of skeletal elements, ectodermal derivatives, muscles and innervation patterns. At the molecular level, the expression of the P-D markers *Hoxa11* and *Hoxa13* was shifted distally, in correlation with the altered P-D identity of skeletal elements. *Meis1* deficient mice, however, do not display defects in stylopod formation (Azcoitia *et al.*, 2005; Hisa *et al.*, 2004), suggesting functional redundancy between *Meis1* and *Meis2*, which show overlapping expression in the limb bud.

Meis transcription factors perform their regulatory activity through the formation of heterodimers with other transcription factors, including Hox proteins, other homeobox transcription factors such as engrailed and PDX1, and non-homeodomain transcription factors such as bHLH- and zinc finger-containing proteins (reviewed in Mann and Affolter, 1998). The main cofactors for *Meis* TFs are members of the PBC subclass of TALE homeobox transcription factors, which comprises the vertebrate *Pbx* genes and their orthologs *extradenticle (exd)* from *Drosophila* and CEH-20 and CEH-40 from *C. Elegans* (reviewed in Bürglin, 1997).

Four different *Pbx* genes have been characterized (Kamps *et al.*, 1990; Monica *et al.*, 1991; Nourse *et al.*, 1990; Popperl *et al.*, 2000). *Pbx1* to *3* are expressed in the mouse limb bud (Capellini *et al.*, 2006; Di Giacomo *et al.*, 2006; González-Crespo *et al.*,

1998, Selleri *et al.*, 2001). Null mutant mice lacking *Pbx1* display malformations affecting the proximal part of the appendages, whereas *Pbx2* null mutants develop normally; however, *Pbx1^{-/-}/Pbx2^{-/-}* double mutants completely lack fore- and hindlimbs, and *Pbx1^{-/-}/Pbx2^{+/-}* show distal limb defects in addition to proximal malformations (Capellini *et al.*, 2006). *In vitro* studies support a role for *Pbx1* as a molecular and functional partner of *Meis* proteins that requires *Meis* for its nuclear import (Capdevila *et al.*, 1999, Mercader *et al.*, 1999, Berthelsen *et al.*, 1999). In the early limb bud, *Pbx1* is expressed in a proximal domain similar to *Meis* genes, and has been proposed to act as the main *Meis* cofactor in this region (Capellini *et al.*, 2006, González-Crespo *et al.*, 1998, Mercader *et al.*, 1999).

Here we describe the effects of overexpressing *Meis1* in distal regions of the developing mouse limb. Our results indicate that *Meis1* inhibits distal limb development and promotes proximalization of limb cell fates. Elimination of *Pbx1* function does not rescue the consequences of *Meis1* overexpression, suggesting either that *Pbx* activity is not required for *Meis1* effects on distal limb development or that the activity of other *Pbx* family members is involved.

Results

Comparative analysis of *Meis1*, *Hoxa11* and *Hoxa13* expression domains

Molecular markers have been described for the three main limb P-D segments: *Meis1* and *Meis2* mark the proximal limb bud regions that give rise to the trunk appendicular structures and the stylopod, *Hoxa11* is expressed in the intermediate limb bud regions that form the zeugopod, and *Hoxa13* labels the autopod

precursor region (reviewed in Tabin and Wolpert, 2007). We have performed a detailed comparative analysis of the temporal and spatial dynamics of *Meis1/Hoxa11/Hoxa13* expression during forelimb development. We performed wholemount *in situ* hybridization on wildtype mouse embryos, which were staged according to somite number. To allow direct comparison of marker gene expression domains, embryos were dissected along the midline with a tungsten needle, and left and right halves were respectively hybridized with *Meis1* and *Hoxa11* or with *Hoxa11* and *Hoxa13* (Fig. 1). The forelimb bud can first be observed as a small protrusion from the trunk at E 9.25. Before this stage, the limb bud mesenchyme expresses *Meis1* ubiquitously. We found that the stage at which a *Meis1*-negative distal domain can be detected is around the 22 somite (s) stage, corresponding to about E9.5 (Fig. 1A). *Hoxa11* can barely be detected at this stage (Fig. 1G). During subsequent stages, the distal *Meis1*-negative domain expands and at the same time a distal domain of *Hoxa11* expression appears that approximately occupies the *Meis1*-free region (Fig. 1B, C, H, I). The *Hoxa11* expression domain expands progressively until E10.5 (Fig. 1J). In the forelimbs of 33s embryos, *Hoxa13* starts to be expressed in a distal-posterior domain nested within the *Hoxa11* expression domain and never overlapping with *Meis1* expression (Fig. 1N). Concomitant with the appearance of *Hoxa13*, *Hoxa11* expression is inhibited in the distal-most portion of the limb, in an area coinciding with the newly formed *Hoxa13* domain (Fig. 1K). During the next two days, the *Hoxa13* domain expands and by E12.5 marks the clearly visible handplate region; in contrast *Hoxa11* expression in E12.5 embryos labels an intermediate segment and *Meis1* is restricted to the proximal-most limb region (Fig. 1F, L, P). Forelimb differentiation has started at this stage of development, and we observe that *Meis1* and

Hoxa11 expression disappears from the limb bud areas where cartilage elements are condensing. During chicken limb development, an initial overlap in the expression domains of *Hoxa11* and *Hoxa13* proteins has been reported (Sato *et al.*, 2007). We performed *in situ* hybridization on adjacent limb sections to study the *Hoxa13* and *Hoxa11*

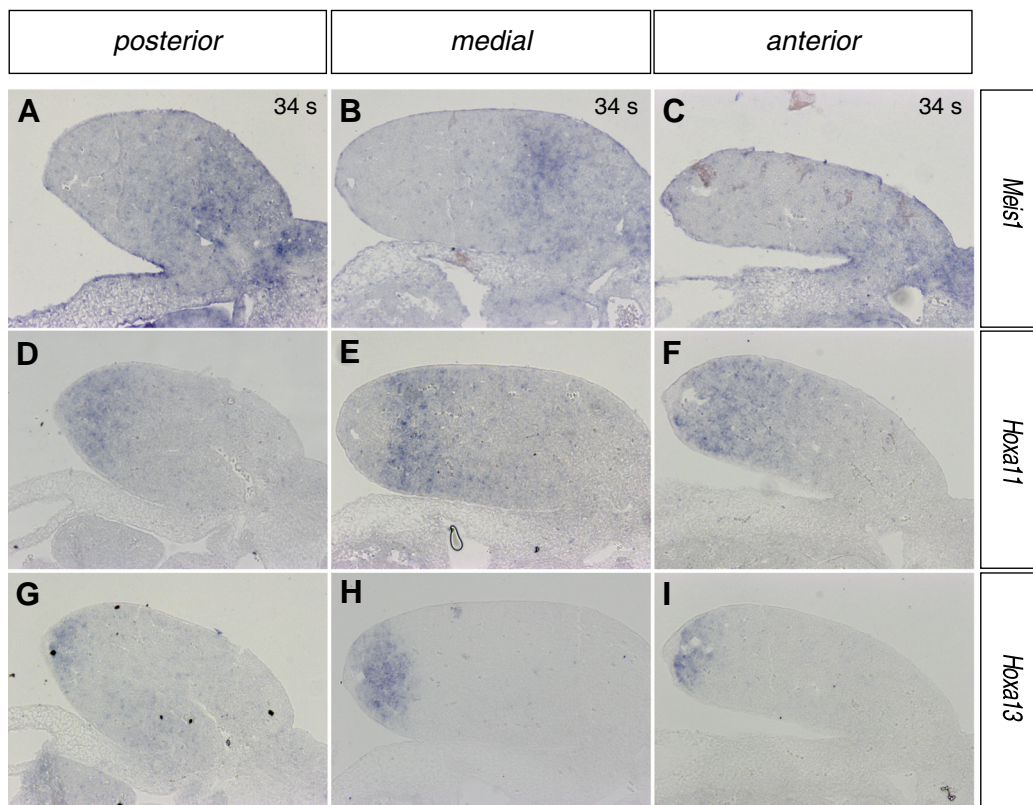


Fig. 2. Detailed analysis of *Meis1*, *Hoxa11* and *Hoxa13* expression domains at the onset of *Hoxa13* expression. *In situ* hybridization on adjacent transversal 34s forelimb sections. Distal is to the left, dorsal to the top. Riboprobes are as indicated on the right of each row. Panels show transverse sections through anterior, medial and posterior limb regions, as indicated at the top of each row. Note that in anterior and posterior sections *Hoxa11* and *Hoxa13* expression domains overlap, whereas in medial positions, their expression domains are nonoverlapping.

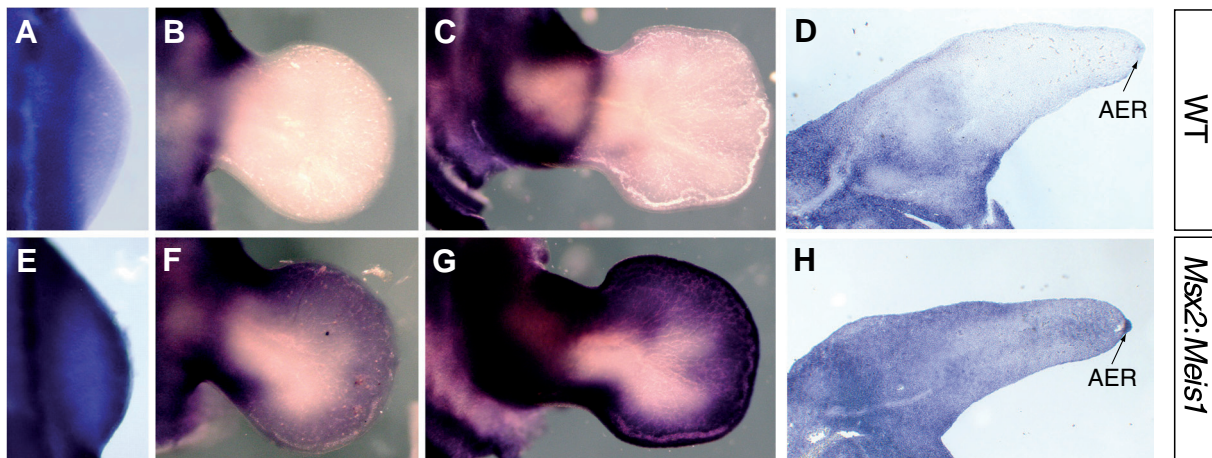


Fig. 3. Ectopic *Meis1* expression in the distal limb bud of *Msx2:Meis1* transgenic limbs. (A,B,C,E,F,G) Wholemount forelimb buds from stages E9.75 (A,E), E11.5 (B,F) and E12.5 (C,G) wildtype (WT) and *Msx2:Meis1* transgenic mice hybridized with *Meis1* antisense mRNA. Anterior is to the top, distal to the right. (D,H) *Meis1* in situ hybridization on transverse sections of E11.5 WT (D) and *Msx2:Meis1* (H) limbs. Note ectopic *Meis1* expression in the apical ectodermal ridge (AER) in H. Dorsal is to the top, distal to the right.

mRNA expression domains in more detail. At the 34s stage, shortly after the onset of *Hoxa13* expression, we observe overlap in the expression of *Hoxa11* and *Hoxa13* domains in the posteriormost and anteriormost limb regions, whereas in more medial parts of the limb their domains are mutually exclusive (Fig. 3). At this stage, *Meis1* and *Hoxa11/Hoxa13* expression domains are mutually exclusive throughout the limb bud. Wholemount ISH at later stages indicates mutual exclusion between *Meis1* and *Hoxa11* domains, and between *Hoxa11* and *Hoxa13* domains (Fig. 1 E, F, K, L, O, P). Our results indicate that *Hoxa11* and *Hoxa13* are transiently co-expressed at least in the anterior and posterior limb regions, while *Meis1* expression does not overlap with either *Hoxa11* or *Hoxa13* at the stages analyzed.

Alteration of zeugopod and autopod development in *Msx2:Meis1* transgenic mice

Two *Meis1* isoforms have been described: *Meis1a* and *Meis1b*. They differ in their C-terminal domains, which contain transactivation functions as well as TSA and PKA responsive elements. The transactivation capacity and response to TSA and PKA is higher for the *Meis1b* C-terminus than for the *Meis1a* C-terminus (Huang et al., 2005). Previous work has shown that *Meis1a* is the predominant isoform at E10.5 (Azcoitia et al., 2005). We therefore decided to use this isoform for the generation of the transgenic mouse lines. To overexpress *Meis1* in the mouse limb, we generated transgenic mice carrying an insert driving *Meis1a* expression under the control of the *Msx2* promoter. The *Msx2* fragment used was a 5.2 kb upstream sequence, which drives transgene expression in the distal limb bud and AER from E9 onwards (Liu et al., 1994). The phenotypic effect of *Meis1* overexpression was first analyzed in transient transgenic embryos. Embryos derived from injected oocytes were fixed at E14.5 and their skeletal elements were analyzed. Limb defects consisting of hypoplasia, retarded ossification, and dysmorphology or absence of zeugopodal and autopodal skeletal elements were observed in 6 out of 31 transient transgenic embryos (Fig. 4 and Table 1; phenotypes are described in detail below). These initial observations prompted us to generate a stable transgenic strain in which

to study the phenotype more in detail. Of 13 transgenic founder mice, one transmitted into the germ line.

Ectopic expression of *Meis1* mRNA was detected in 84% (n=47/56) of embryos from the stable transgenic line. We observed differences in the levels of ectopic *Meis1* expression, even among embryos of the same litter. Around one third of the transgenic embryos displayed higher levels of ectopic *Meis1* expression (data not shown). This difference in gene expression might account for the difference in phenotypic penetrance observed in embryos of Tg/+ X +/+ crosses (see below). We observed that, instead of the proximal restriction found in wildtype embryos (Fig. 3A-C), *Meis1* expression expands into the distal limb bud region in transgenic limb buds (Fig. 3D-F). From E9 to E10.5, the whole limb bud is *Meis1*-positive (Fig. 3D). Later, ectopic *Meis1* expression in the mesenchyme is confined to a distal portion of the limb bud, underlying the AER (Fig. 3E). At E12.5, ectopic *Meis1* can be observed in the AER and the interdigital zones (Fig. 3F). We observed some disparities between the expected expression driven by the *Msx2* promoter and the actual expression of ectopic *Meis1* observed in the transgenic limb buds. In the chick, we have previously observed that implants of cells overexpressing *Meis1* in the distal limb tend to relocate to more proximal positions (Mercader et al., 2000). A similar phenomenon has also been observed during regeneration of urodele limb appendages (Mercader et al., 2005). The fact that the distribution of *Meis1*-positive cells in the distal limb region does not completely fit the *Msx2* promoter activity could be a conse-

TABLE 1

DISTRIBUTION OF PHENOTYPES IN *MSX2:MEIS1* TRANSGENIC ANIMALS

Phenotype	transient transgenics	transgenic line	Tg x Tg crosses
none	81% (25/31)	80% (35/44)	27% (16/59)
mild	10% (3/31)	11% (5/44)	17% (10/59)
intermediate	3% (1/31)	7% (3/44)	36% (21/59)
strong	6% (2/31)	2% (1/44)	20% (12/59)

quence of altered adhesive properties of *Meis1*-overexpressing cells; however, we do not have direct evidence for this from the present study. Other sites of ectopic *Meis1* expression included the retina, craniofacial mesenchyme, the dorsal roof of the mid-brain, the hindbrain, the neural tube, and the ectomesenchyme of the dorsal midline (not shown).

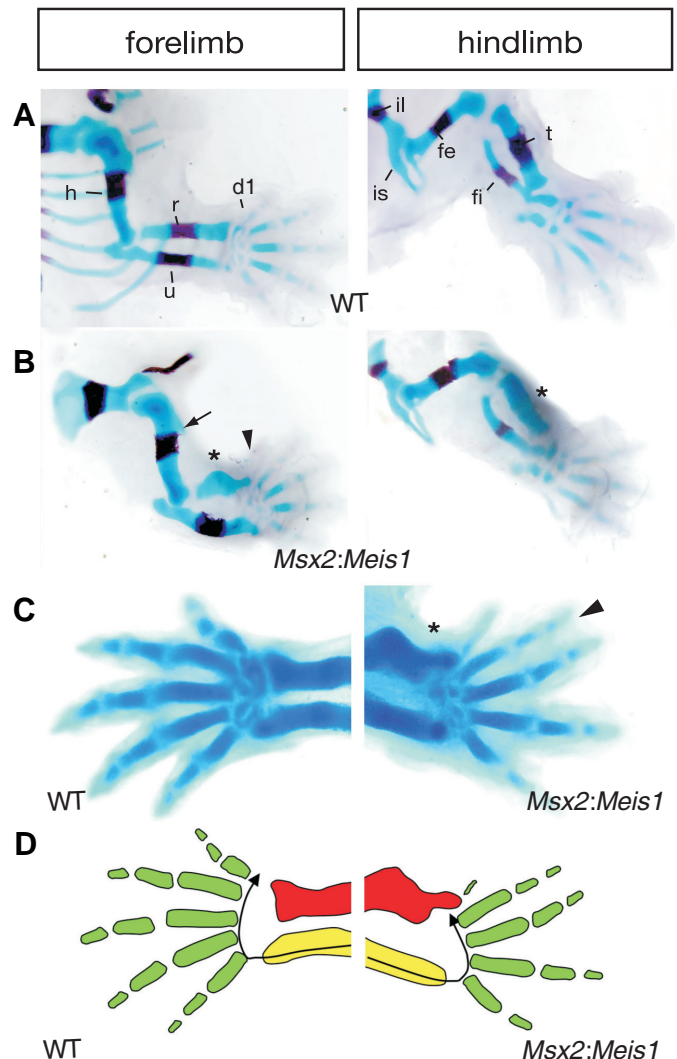
We further investigated the effect of ectopic *Meis1* expression on limb development by analyzing the limb skeletal phenotypes of E17.5 fetuses of the stable line carrying the *Msx2:Meis1* transgene (Tg). Alterations affecting zeugopod and autopod elements were detected in 20% of embryos obtained from Tg/+ X +/+ crosses and 73% of embryos derived from Tg/+ inter-crosses (Table I). We classified the observed phenotypes into three classes according to their severity in forelimbs (Table I and Fig. 5). Mild phenotypes mainly affected the zeugopod and were characterized by delayed ossification and moderate anterior bending of the radius (Fig. 5B). Ossification of autopod elements was also slightly delayed in this class. Intermediate phenotypes showed a longer delay in radius ossification and a very notable dysmorphology of this element, which was strongly bent and reduced. The ulna was also reduced and displayed delayed ossification (Fig. 5C). The autopodal phenotype in this class was also characterized by delayed cartilage condensation and ossification, which especially affected anterior digits (Fig. 5C). Finally, strong phenotypes were characterized by an absence of anterior autopod elements. This typically involved the total absence of the anterior carpals, partial or total absence of metacarpal 1 and the complete absence of digit 1 (Fig. 4B, C, D, 5D). Concomitantly, the radius extended into the areas that would normally have been occupied by the missing elements (Fig. 3B, C, D, 5D). Specimens with strong phenotypes also displayed syndactyly of the soft tissues between digits 1 and 2 or 2 and 3 (Fig. 4C and 5D). There is a good correlation between the phenotypes in forelimbs and those observed in hindlimbs, although the hindlimb phenotypes appear to be less severe. The tibia and fibula were reduced in hindlimbs, and, as described for the forelimb, cartilage condensation of the autopod was retarded; however, ectopic condensation of zeugopodal elements or absence of autopodal elements was never observed (Fig. 4B, C, Fig. 5B, C, D). In the progeny of

Msx2:Meis1 heterozygous inter-crosses, there was a high incidence of strong phenotypes (Table I). Although the development of stylopod elements was generally unaffected in *Msx2:Meis1* transgenics, in specimens of the intermediate and strong forelimb phenotypic classes the humerus lacked the deltoid tuberosity (Fig. 5B, C). This phenotype was not observed, however, in any of the transient transgenic specimens (Fig. 4B). We therefore cannot definitively link this stylopod phenotype to *Meis1* overexpression, because it could be an artefactual consequence of the integration site in the single stable transgenic line.

Hoxa11 and *Hoxa13* expression in *Msx2:Meis1* transgenic embryos

To analyze the effect of ectopic *Meis1* on limb P-D markers we investigated the expression of the zeugopod and autopod markers *Hoxa11* and *Hoxa13* in *Msx2:Meis1* transgenic limb buds at different stages of limb development. We found that the somite stage at which *Hoxa11* and *Hoxa13* expression starts is unchanged in *Msx2:Meis1* in comparison with wildtype siblings of the same somite number (not shown). At E11, however, the *Hoxa11* expression domain was shifted distally in *Msx2:Meis1* limbs (Fig. 6A, C). The same effect was observed in E12.5 and

Fig. 4. *Meis1* overexpression interferes with the development of zeugopod and autopod skeletal elements. Limb skeletal preparations of transient *Msx2:Meis1* transgenic embryos at E14.5. (A) Wildtype littermate. (B) Example of an *Msx2:Meis1* transgenic limb with a strong phenotype. Note the absence of ossification of the radius and tibia (asterisks) and the anterior bending of the radius. Arrowhead in (B) indicates absence of digit 1 cartilage condensations. Arrow marks the deltoid tuberosity of the stylopod, which is unaffected. (C) Close-up views of the distal forelimb of a wildtype littermate and a second *Msx2:Meis1* transgenic with a strong phenotype. Note the invasion of the radius into the handplate (asterisk), which is accompanied by reduced formation of digit 1 phalanges. Additionally, this specimen reveals syndactyly of digits 2 and 3 (arrowhead). (D) Schematic representation of defects in distal bone formation observed in *Msx2:Meis1* transgenic forelimbs. The ulna is depicted in yellow, the radius in red and the autopod cartilage elements in green. In the presence of ectopic *Meis1* expression, invasion of the radius into handplate regions seems to displace anterior autopod elements or interfere with the differentiation wave of autopod cartilage elements, which goes from posterior to anterior. d, digit; fe, femur; fi, fibula; h, humerus; il, ilium; is, ischium; r, radius; t, tibia; u, ulna.



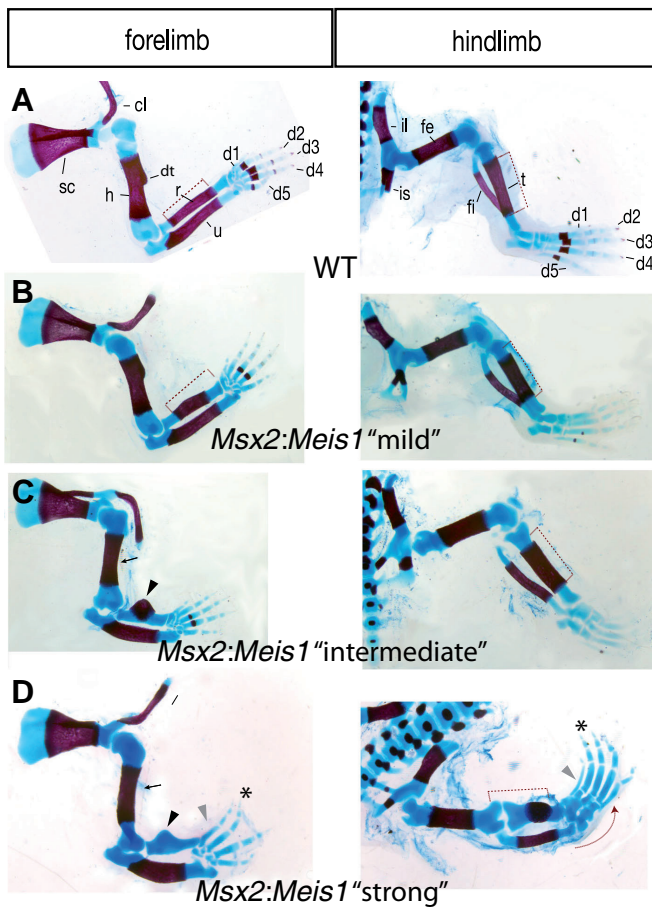


Fig. 5. Defects in distal limb development in a stable *Msx2:Meis1* transgenic line. Skeletal preparations of E17.5 wildtype (WT) (A) and *Msx2:Meis1* (B,C,D) fore- and hindlimbs. Since the *Msx2:Meis1* phenotype showed varying penetrance, embryos were classified into three groups as indicated (B,C,D). (B) Forelimbs of the “mild” phenotype group show reduced ossification of the radius, sometimes accompanied by slight bending. Similarly, hindlimbs show reduced ossification of the tibia compared to same-staged WTs. The red bars are shown to aid comparison of ossified radius length between WT and transgenic limbs. Black arrowheads in (C,D) indicate a strongly reduced or absent radial ossification center and bending of the radius. Grey arrowheads mark missing d1 in the forelimb and strongly reduced d1 in the hindlimb. Asterisks mark fused digits 2 and 3. Arrows highlight missing deltoid tuberosities. Red arrow in (D) indicates a ventral bending of the hindlimb. cl, clavicle; d, digit; dt, deltoid tuberosity; fe, femur; fi, fibula; h, humerus; il; ilium; is, ischium; r, radius; sc, scapula; t, tibia; u, ulna.

E13 limb buds, with the displacement more evident at the anterior zeugopod/autopod boundary (Fig. 6B, D). Concomitantly, the *Hoxa13* expression border was displaced distally, especially in its anterior-most region, coinciding with the anterior wrist elements and the metacarpal/digit 1 precursor area, which is the same region in which *Hoxa11* shows a more evident distal displacement (Fig. 6E, G). In addition, the *Hoxa13* expression signal was slightly fainter overall than in wildtype limb buds (Fig. 6G, H). The reduction in the *Hoxa13* expression domain and the shift in the anterior distal border thus correlated with an expansion of the *Hoxa11* expression domain towards exactly this region (Fig. 6I-L). This shift in expression, however, occurs in the absence of an

overall change of limb morphology at these stages and cannot be attributed to a delay in limb development, because the timing of P-D marker activation remained unchanged (not shown).

***Pbx1* loss-of-function does not rescue the *Msx2:Meis1* phenotype**

In all functional contexts studied so far *Meis* and *Pbx* transcription factors act in concert to modulate the activity of other transcription factors. The expression pattern of *Pbx1* correlates with the *Meis1* proximal limb expression domain, suggesting that *Pbx1* cooperates with *Meis1* during vertebrate limb development. To determine whether the alterations induced by *Meis1* overexpression require interaction with *Pbx1*, we crossed the *Msx2:Meis1* line into a *Pbx1* null mutant line (Selleri *et al.*, 2001), which was backcrossed towards a C57BL/6 background. Attenuation of the *Msx2:Meis1* limb phenotype by *Pbx1* deficiency would indicate a cooperative action of *Meis1* with *Pbx1* in the observed alterations of distal limb development.

We performed seven crosses, which yielded a total number of 45 embryos. Embryos were stained with Alcian blue and Alizarin red to visualize limb skeletal elements (Fig. 6). *Pbx1*^{-/-} embryos displayed several malformations affecting the stylopod, such as fused scapula and humerus bones and loss of the deltoid tuberosity of the humerus. Similarly, in the hindlimb the coxae-femur articulation appeared to be fused (Fig. 7B). Compared with the *Msx2:Meis1* line, *Msx2:Meis1/Pbx1* crosses showed a reduced intensity of the *Meis1* overexpression phenotype, with only phenotypes of the “mild” class observed. The severity of the mutant phenotypes was similar in *Msx2:Meis1/Pbx1*^{-/-} (N=3), *Msx2:Meis1/Pbx1*^{+/-} (N=12), and *Msx2:Meis1/Pbx1*^{+/+} (N=6) limbs (Fig. 7C, D), indicating that it is the genetic background that attenuates the *Msx2:Meis1* phenotype, and not the absence of *Pbx1* function *per se*. These results thus suggest that *Pbx1* elimination does not alter the *Msx2:Meis1* phenotype and is thus not required for *Meis1*-induced distal limb defects.

In the E9.5 murine limb bud, *Pbx1* shows a nuclear expression pattern in the proximal limb region corresponding to the *Meis* expression domain (González-Crespo *et al.*, 1998; Mercader *et al.*, 1999). Immunohistochemistry with antibodies against *Pbx1a*, *Pbx1b* and a C-terminal motif common to *Pbx1*, *Pbx2* and *Pbx3* did not reveal any clear differences between nuclear *Pbx* expression domains in wildtype and transgenic limbs at stages between E10 and E11.5 (Fig. 7B, F and data not shown). Thus, in agreement with the results presented above, we found that ectopic *Meis1* expression does not extend the proximal pattern of *Pbx1* nuclear expression into distal limb regions (Fig. 8).

Discussion

Ectopic Meis1 overexpression interferes with distal limb development

We have previously shown that *Meis1* is a molecular marker of the stylopod, and that its ectopic expression throughout the chicken limb bud leads to alterations of zeugopod and autopod elements without affecting the development of the proximal limb parts (Mercader *et al.*, 1999). Here we report similar effects on skeletal patterning obtained by overexpressing *Meis1* in the mouse limb primordium. As with the chicken limb, the observed defects include changes to the P-D identity of limb cells, as shown

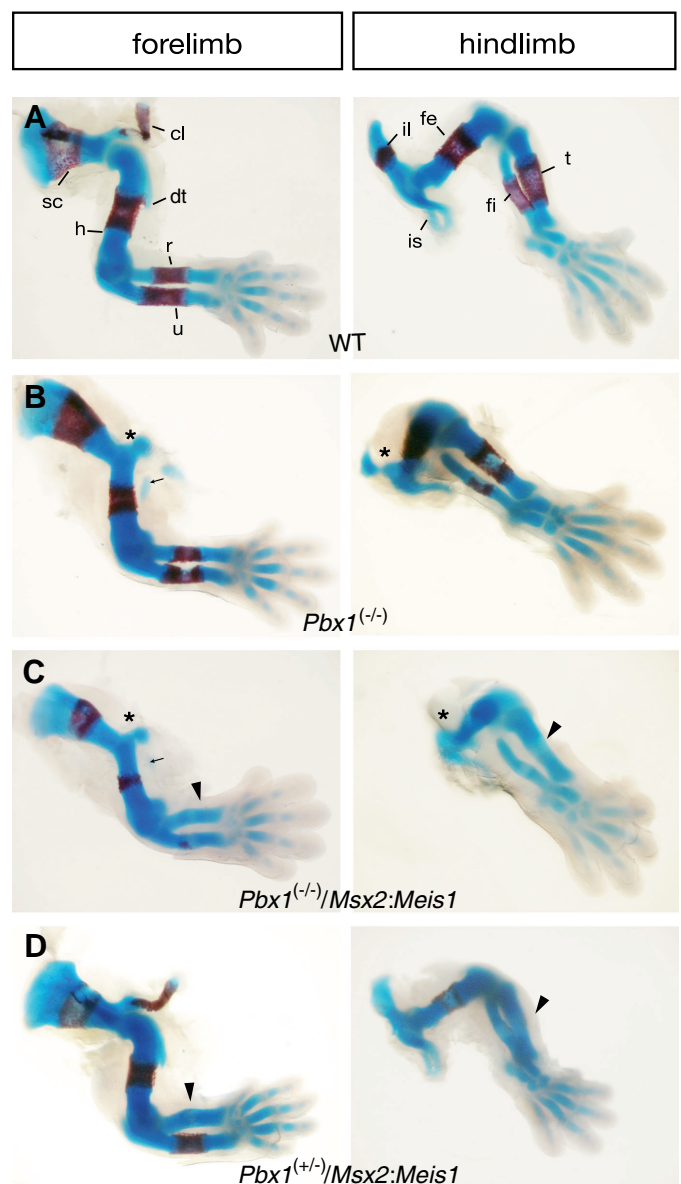
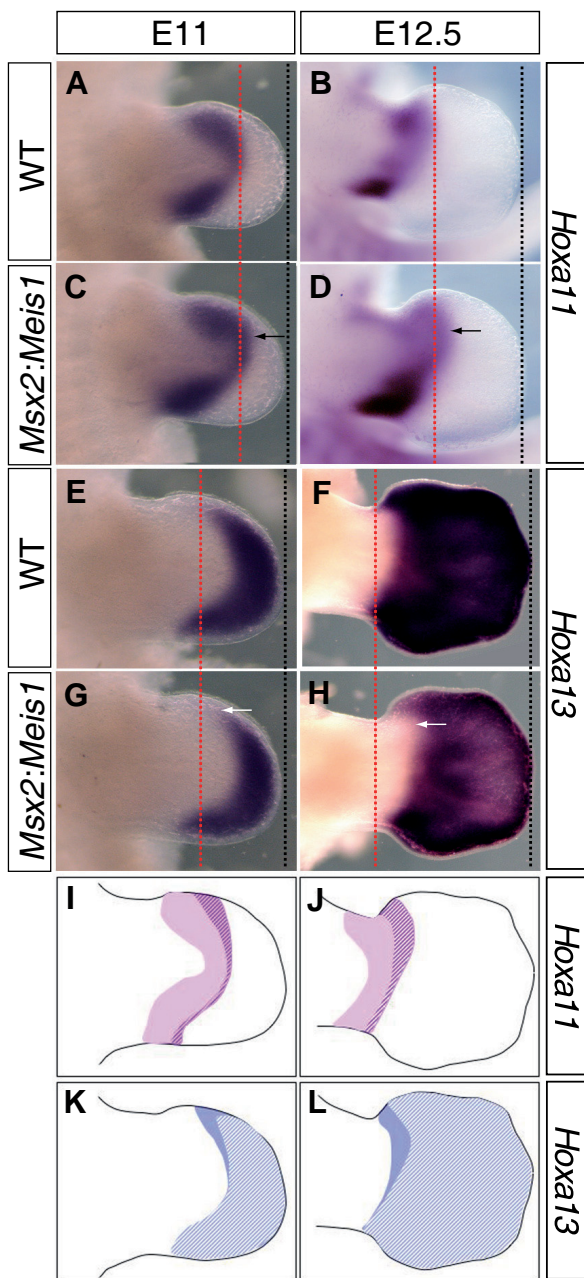


Fig. 6 (Left). Ectopic *Meis1* expression leads to a distal shift of *Hoxa11* and *Hoxa13* expression domains. Wholemount in situ hybridizations of *Hoxa11* and *Hoxa13* in E11 and E12.5 limb buds. **(A-D)** Compared with a wildtype (WT) forelimb (A), the *Hoxa11* expression domain in *Msx2:Meis1* forelimbs is shifted distally (C, arrow). This distal extension is maintained at later stages of development and is not exclusive to the forelimb, since it is also observed in hindlimb buds at E12.5 (D, arrow). Red dotted lines mark the distal border of the *Hoxa11* expression domain in WT limb buds. **(E-H)** The *Hoxa13* expression domain in *Msx2:Meis1* limbs is, in contrast, reduced compared with WT littermates. Red dotted lines mark the proximo-anterior *Hoxa13* expression limit in WT embryos. Note that this limit is shifted distally in *Msx2:Meis1* limbs (white arrows). In all panels, black dotted lines highlight the tip of the limb bud. **(I-L)** Schematic illustration of the shift in *Hoxa11* and *Hoxa13* expression domains observed in the presence of ectopic *Meis1* in the distal limb bud. Filled colored areas represent the normal *Hoxa11* and *Hoxa13* expression domains; striped areas represent *Hoxa11*/*Hoxa13* expression domains in *Msx2:Meis1* transgenic limbs. In transgenic limbs the *Hoxa11* domain is shifted distally. At the same stages, cells located at the proximal border within the WT *Hoxa13* expression domain stop expressing it in the transgenics, thus undergoing a change in proximodistal marker gene expression. The effect is more prominent in the anterior limb bud.

domain in *Msx2:Meis1* forelimbs is shifted distally (C, arrow). This distal extension is maintained at later stages of development and is not exclusive to the forelimb, since it is also observed in hindlimb buds at E12.5 (D, arrow). Red dotted lines mark the distal border of the *Hoxa11* expression domain in WT limb buds. **(E-H)** The *Hoxa13* expression domain in *Msx2:Meis1* limbs is, in contrast, reduced compared with WT littermates. Red dotted lines mark the proximo-anterior *Hoxa13* expression limit in WT embryos. Note that this limit is shifted distally in *Msx2:Meis1* limbs (white arrows). In all panels, black dotted lines highlight the tip of the limb bud. **(I-L)** Schematic illustration of the shift in *Hoxa11* and *Hoxa13* expression domains observed in the presence of ectopic *Meis1* in the distal limb bud. Filled colored areas represent the normal *Hoxa11* and *Hoxa13* expression domains; striped areas represent *Hoxa11*/*Hoxa13* expression domains in *Msx2:Meis1* transgenic limbs. In transgenic limbs the *Hoxa11* domain is shifted distally. At the same stages, cells located at the proximal border within the WT *Hoxa13* expression domain stop expressing it in the transgenics, thus undergoing a change in proximodistal marker gene expression. The effect is more prominent in the anterior limb bud.

Fig. 7 (Right). Skeletal preparations of *Pbx1*^{(-/-)/*Msx2:Meis1*} double mutant fore- and hindlimbs. **(A)** Skeletal fore- and hindlimb preparations from a wildtype E14.5 sibling. **(B)** Same-staged preparations of *Pbx1*^(+/-) limbs; the forelimbs display fused scapula - humerus joints and the femur is fused to the hip (asterisks). Additionally, the deltoid tuberosity is missing (arrow). **(C)** *Pbx1*^{(+/-)/*Msx2:Meis1*} limbs still display *Pbx1*^(+/-) specific defects and additionally show mild *Msx2:Meis1* phenotypes (slightly bent radius and delayed ossification of radius and tibia, arrowheads). **(D)** *Pbx1*^{(+/-)/*Msx2:Meis1*} limbs display features typical of a mild *Msx2:Meis1* phenotype, as observed in (C). cl, clavicle; d, digit; dt, deltoid tuberosity; fe, femur; fi, fibula; h, humerus; il, ilium; is, ischium; r, radius; t, tibia; sc, scapula; u, ulna.

by the altered expression of P-D markers and the extension of limb structures to positions distal to their normal location.

We observed a distal shift of the borders of the two markers that define the zeugopod and autopod, *Hoxa11* and *Hoxa13* (Fig. 6I-L). The expression domains of these markers first appear at the postero-distal tip of the limb bud and progressively expand, displacing the borders to more proximal positions. Our results might therefore indicate only a general delay in limb development. Against this possibility, however, we observed that the timing of *Hoxa11* and *Hoxa13* activation is unchanged in the transgenic embryos. We therefore favor the view that ectopic *Meis1* changes the ability of distal limb cells to progress in distalization. The shift of the expression domains is initially observed across the whole limb bud and affects the proximal *Hoxa11* expression border as well as its distal border, which coincides with the proximal limits of *Hoxa13* expression. At later stages, however, only the anterior areas of the boundary between zeugopod and autopod retain the shifted expression patterns of *Hoxa11* and *Hoxa13*, and it is only around this area that we observed a skeletal condensation pattern compatible with a P-D shift in skeletal elements. Overexpression of *Meis1* in the chick limb bud triggered a very similar alteration at the anterior zeugopodal/autopodal boundary (Mercader et al., 1999), indicating that this area is especially sensitive to alterations in P-D specification mechanisms. This autopodal region is quite unique, as it only expresses one Hox gene, namely *Hoxa13*. Digit 1 is specifically underdeveloped in mice with one dose of *Hoxa13* and is the only digit lost in the complete absence of *Hoxa13*. Furthermore, a deletion of one copy of the complete *Hoxa* gene cluster specifically removes only digit 1 (Fromental-Ramain et al., 1996, Kmita et al., 2005). The fact that the development of the most anterior autopod relies mostly on the

activity of a single Hox gene might underlie the enhanced susceptibility of this region to pattern alterations in general and to *Meis1* gain of function in particular. Some of the effects of *Meis1* overexpression in the distal limb could be in fact explained by the reduction in *Hoxa13* expression levels and/or alterations in HoxA13 protein activity, since *Hoxa13*^{+/-} mice also show fusion of digits 2 and 3 (Stadler et al., 2001) and *Hoxa13* deficient mice show distally-extended *Hoxa11* expression in limb buds (Post and Innis, 1999).

During early limb development *Meis1* and *Hoxa11* need to establish mutually exclusive domains. Our results may thus reflect a physiological role for *Meis1* in restricting 5' *Hox* gene expression to distal limb regions, and this *Meis1* function may operate at different levels. Meis/Pbx activity has been shown to regulate the transcription of *Hoxb2* by directly modulating the transcriptional activity of *Hoxb1* protein in a cross-regulatory loop (Jacobs et al., 1999). It may be that a similar regulatory loop occurs in the limb bud, whereby *Meis1* directly regulates the protein and/or transcriptional activity of *Hoxa11* and *Hoxa13*. Previous studies have also demonstrated that a distal limb enhancer, located remotely upstream of the *Hoxd* complex, drives 5' *Hoxd* gene expression in the autopod during embryogenesis (Spitz et al., 2003). A similar expression control mechanism has been proposed for the *Hoxa* cluster (Lehoczky et al., 2004). Therefore, a second possible explanation is that the observed alterations in the transition of *Hoxa11* to *Hoxa13* expression could be caused by an influence of *Meis1* activity on the distal limb enhancer.

In addition to the observed alterations to the establishment of P-D identities, the limbs of *Meis1* transgenic mice show defects in bone growth and differentiation. It is important to note that during normal development *Meis* expression is downregulated in chondrogenic centres. Therefore, the alterations in bone differentiation observed after *Meis1* overexpression could be due to a direct counteraction of this process by *Meis* activity. However, if this was the case, we would expect to see alterations in bone formation within all P-D limb segments after *Meis1* overexpression, which is not observed. Overexpression of *Meis1* in the chick induces bone differentiation defects only in the skeletal elements of the distal limb; the stylopod was unaffected. This suggests that the alterations in bone differentiation derive from misspecification of skeletal elements rather than from an interference of *Meis* activity with the ossification program. The results reported here support this hypothesis, as *Meis1* overexpression in *Msx2:Meis1* transgenic mouse limb buds is specific for undifferentiated cells, there being therefore no *Meis1* overexpression during skeletal element differentiation. Under these conditions the transgenic *Msx2:Meis1* mice reproduce the distal-specific growth and differentiation defects observed in the chick. This indicates that these defects are caused by alterations early in the specification process, when cells are still in the undifferentiated area under the influence of the AER. Thus the provision of altered positional cues to precursors of the primary chondrogenic centers may result in alterations of

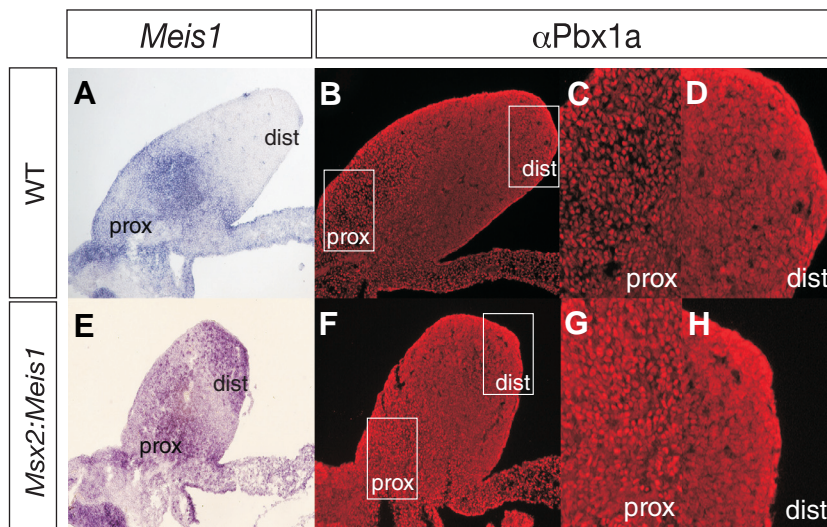


Fig. 8. Overexpression of *Meis1* does not alter *Pbx1* subcellular distribution in the limb bud. *Meis1* mRNA in situ hybridization and *Pbx-1* immunohistochemistry on adjacent limb cryosections from E10.5 wildtype (A-D) and *Msx2:Meis1* transgenic (E-H) mice. Anterior is to the left, distal to the top. (C,G) and (D,H) are zoomed images of the proximal and distal regions indicated in (B and F), respectively: dist, distal; prox, proximal. Note that whereas *Meis1* expression is ectopically expanded to more distal parts of the limbs (E) in *Msx2:Meis1* transgenics, the nuclear pattern of *Pbx1* staining was restricted to the proximal limb bud both in wildtypes (B-C) and in transgenic littermates (F-G); no distal expansion of its expression domain could be observed (D,H).

the differentiation program that only become apparent during the subsequent growth and differentiation phase. Similar observations have been reported after the modification of *Hox* gene activity. *5'Hoxd* and *5'Hoxa* genes are expressed at specific A-P and P-D positions of the limb bud (Dollé *et al.*, 1989, Nelson *et al.*, 1996, Yokouchi *et al.*, 1991). At the onset of cartilage condensation, *Hox* gene expression becomes downregulated (Suzuki and Kuroiwa, 2002). Nevertheless, gain or loss of function in *Hox* gene activity leads to position-specific defects in bone differentiation, suggesting that early misspecification leads to differentiation defects (Davis and Capocchi, 1996, Fromental-Ramain *et al.*, 1996, Goff and Tabin, 1997, Morgan *et al.*, 1992, Zakany and Duboule, 1999).

Hoxd13 and *Hoxd12* misexpression in the limb bud interferes with the correct development of zeugopodal elements of chicken and mouse embryos, respectively (Goff and Tabin, 1997, Knezevic *et al.*, 1997). *Hoxd13* overexpression leads to shorter tibia and fibula bones and *Hoxd12* gain-of-function in the posterior lateral plate mesoderm leads to hemimelia of the tibia. Similarly, misexpression of another distal *Hox* gene, *Hoxa13*, also leads to development of shorter zeugopodal elements (Yokouchi *et al.*, 1995). A possible explanation is that these *Hox* genes, which are predominantly or exclusively expressed in the autopod region, interfere with the *Hox* gene of protein function within the zeugopod when overexpressed. *Hoxd13* a13 d12 might interfere with the function of other *Hox* genes such as *Hoxd11* and *Hoxa11*, which have been shown to control zeugopod development (Davis *et al.*, 1995). Given that *Meis1* overexpression causes zeugopodal defects that partially resemble those found in *Hoxd13*, *Hoxd12* or *Hoxa13* overexpression, but does not activate these distal genes in the autopod, it might act in this context by interfering with the correct Hox protein function in the zeugopod.

In the proximal limb, *Meis1* expression is promoted by RA, which has been proposed as a determinant of proximal limb identities (Mercader *et al.*, 2000b, Ribes *et al.*, 2007, Yashiro *et al.*, 2004). The phenotype obtained after *Meis1* overexpression partially resembles the teratogenic effects of RA on limb development (Sucov *et al.*, 1995, Yashiro *et al.*, 2004). A closely related gene of the *Meis* family, *Meis2* (Ceconi *et al.*, 1997, Oulad-Abdelghani *et al.*, 1997), is coexpressed with *Meis1* during proximal limb development, is also regulated by RA and probably performs redundant roles with *Meis1*. We therefore suggest that *Meis1* and *Meis2* might be important mediators of the RA function and teratogenic effects during limb P-D specification.

***Meis* proteins might act independently of a *Pbx* cofactor**

The TALE homeobox proteins *Meis* and *Pbx* have been shown to form heterodimers and to act as a functional unit in several species and cellular contexts. The nuclear localization of these proteins has also been shown to be interdependent (Abu-Shaar *et al.*, 1999, Berthelsen *et al.*, 1999, Capdevila *et al.*, 1999, Mercader *et al.*, 1999, Rieckhof *et al.*, 1997). In *Drosophila*, the *Pbx* ortholog EXD translocates to the nucleus only in presence of the *Meis* ortholog HTH. In other species, however, the role for nuclear transport seems to be switched between *Meis* and *Pbx* proteins (Maeda *et al.*, 2002, Prpic *et al.*, 2003, Vlachakis *et al.*, 2001). For example, in the spider, *exd* is expressed exclusively in the proximal limb, whereas *hth* is expressed throughout the appendage; however, HTH is localized in the nuclei only of

proximal cells, and shows cytoplasmic expression in distal regions. Similarly, during hindbrain development in the zebrafish, *Pbx4* regulates nuclear transport of *Meis3* (Choe *et al.*, 2002). We previously reported that *Pbx1* nuclear expression is limited to a proximal limb region that coincides with the *Meis* expression domain (González-Crespo *et al.*, 1998). A distal cytoplasmic signal detected with anti-*Pbx1* antibody was then interpreted as indicating the presence of cytoplasmic *Pbx1* protein in the distal limb. A recent report, however, showed restriction of *Pbx1* transcripts to the proximal limb (Capellini *et al.*, 2006), suggesting that the cytoplasmic antibody staining for *Pbx1* in the distal limb was unspecific. We have now tested this by comparing the distal limb cytoplasmic staining between WT and *Pbx1*-deficient embryos at E11.5 and found that indeed the distal cytoplasmic signal observed at this stage is unrelated to *Pbx1* protein (not shown). Nonetheless, activation of nuclear *Pbx* in the distal limb bud, detected with an antibody to *Pbx1*, 2, and 3, was reported after ectopic PKA activation (Kilstrup-Nielsen *et al.*, 2003). In order to determine whether ectopic *Meis1* activity in the *Msx2:Meis1* transgenic line might lead to a similar distal expansion of nuclear *Pbx* expression in the limb bud, we analyzed the changes in *Pbx* antibody staining. However, *Pbx* expression was unaffected, suggesting that additional signaling events, such as PKA signaling, are required to ectopically express *Pbx* in distal limb domains.

Finally, we found that elimination of *Pbx1* does not rescue the *Meis1* overexpression phenotype, indicating either that *Meis1* is able to perturb P-D limb specification in the absence of any *Pbx* function or that ectopic *Meis1* recruits other *Pbx* proteins to produce this overexpression phenotype. Other *Pbx* genes expressed in the developing limb include *Pbx2* and *Pbx3* (Capellini *et al.*, 2006, Di Giacomo *et al.*, 2006). While *Pbx3* is not expressed in all limb regions at the relevant stages, *Pbx2* is expressed throughout the limb bud during the P-D specification phase and is functionally involved in both proximal and distal limb patterning together with *Pbx1* (Capellini *et al.*, 2006). We cannot, therefore, rule out an interaction between *Pbx2* and *Meis1* in the generation of the *Meis1* overexpression phenotype. Functional studies involving crosses of *Msx2:Meis1* transgenics into the *Pbx2* null mutant line will hopefully answer this question in the future.

Materials & Methods

Generation of *Msx2:Meis1* transgenic lines

A full-length *Meis1a* cDNA fragment was cloned into the EcoRI and SacI sites of the pPGKneobpA expression vector. A + 0.52 kb *Msx2* promoter fragment was inserted at the EcoRI site upstream of the *Meis1a* ATG start codon. A larger fragment of the *Msx2* promoter was subsequently cloned into SpeI/XhoI restriction sites, to yield a total promoter length of 5.2 kb.

For injection, the plasmid was linearized with XhoI followed by purification by electroelution. The plasmid was further purified by three phenol extractions followed by three ether extractions. The plasmid was ethanol precipitated successively three times and resuspended in Tris-EDTA buffer (7mM Tris pH 7.4; 0.2mM EDTA). As a last step, the plasmid was purified by dialysis for 72 h.

Transient transgenic embryos were generated by microinjecting the linearized construct into fertilized C57/BL6 oocytes. A transgenic mouse strain was derived from one of the founder animals; these animals have the characteristic *Meis1*-overexpression phenotype of shortened forelimbs with digits 2 and 3 fused.

The *Msx2:Meis1* stable transgenic line was generated on a C57B6CBA

genetic background and subsequently backcrossed into C57B6 for six generations. Embryos from generations F1 to F6 were used for these studies.

For genotyping, genomic DNA was extracted from mouse tails or embryonic vitelline membranes. RT-PCR was performed using primers tg-Forward: GAC GAC CTA CCC CAT TAT and tg-Reverse: CTC TCT GGC TCC CTT CCT ACT. As a further control, embryo heads were hybridized with *Meis1* to detect ectopic *Meis1* expression in midline and branchial arches of *Msx2:Meis1* embryos.

To generate *Msx2:Meis1/Pbx1* (-/-) mutant embryos, *Msx2:Meis1* transgenic mice displaying a strong phenotype were crossed with *Pbx1*(+/-) mice. Littermates from seven crosses (n=45) were genotyped and processed for cartilage staining.

In situ hybridization

Embryos were fixed overnight in 4% paraformaldehyde (PFA). Whole-mount *in situ* hybridization was performed as described (Wilkinson and Nieto, 1993). For *in situ* hybridization on sections, fixed embryos were transferred to 30% sucrose in PBS and embedded in OCT. Cryosections (10 to 15 μ m) were collected on Superfrost slides and allowed to air-dry for 2 h. Before hybridization, slides were washed for 5 min with PBS and refixed for 10 min with 4% PFA. Slides were washed for 5 min in PBS and prehybridized for 5 min at 65°C in prehybridization buffer (50% formamide, 1x SSC pH 4.5, 1% SDS). For each slide, 2 μ l riboprobe reaction mix was diluted in 100 μ l hybridization buffer (11.4 g NaCl, 1.4 g Tris-HCl pH 7.5, 0.134 g Trisbase, 5 mM NaH₂PO₄·2 H₂O, 5 mM Na₂HPO₄, 0.05 M EDTA, 50% formamide, 10% dextran sulfate, 1 mg/ml tRNA, 1x Denhardt's solution). After overnight hybridization at 70°C, slides were transferred to a slide rack and placed in a jar containing preheated posthybridization buffer (50% formamide, 1x SSC pH 4.5, 1% SDS). After two 30 min washes at 65°C, the rack was cooled to room temperature (RT) and slides washed twice for 30 min in MABT (100 mM maleic acid, 150 mM NaCl, 0.1% Tween20, pH 7.5). Prior to antibody incubation, sections were blocked for 1 h at RT in blocking solution (2% blocking reagent (Roche) and 20% goat serum in MABT). For antibody incubation, anti-DIG-AP (Roche) was diluted 1/2000 in blocking solution and 200 μ l were added per slide. Slides were incubated overnight at RT, and then washed 5 x 20 min at RT in MABT. Slides were next washed 2 x 10 min with gentle rocking in AP buffer (100 mM Tris HCL pH 9.5; 150 mM NaCl, 50 mM MgCl₂, 0.1% Tw20; 0.5 mg/ml levamisol). For the staining reaction, 200 μ l BM Purple staining solution (Roche) were added to each slide. The staining reaction required from a few hours to 2 days. When necessary, the staining solution was replaced every 12 h. The reaction was terminated by a rapid rinse in H₂O, and slides were mounted in Aquatex (Merck). For probe synthesis of *Hoxa11* and *Hoxa13*, PCR products comprising sequences between (-25 bp to +506 bp) and (-541 bp to +478 bp) respectively were used as templates. *Meis1a* riboprobe spanned the sequence between 814 bp and 2119 bp.

Immunohistochemistry

For cryosectioning, embryos were fixed overnight in 4% PFA, soaked overnight in 30% sucrose/PBS solution and embedded in OCT. 12 μ m sections were collected on Fisher Superfrost slides. Sections were air-dried for 30 min and refixed in ice-cold acetone for 2 min at 4°C. Slides were then immediately transferred to a jar containing 0.1% Tween 20 in PBS (PBT) and washed three times for 5 min each. Permeabilisation was increased by a 10 min wash in 0.05% TritonX-100 in PBS. Sections were preincubated for 1 hour at RT in blocking buffer (10% goat serum in PBT) and incubated overnight in primary antibody diluted in 2% goat serum in PBT. Sections were then washed three times for 5 min in PBT. The secondary antibody was biotin conjugated anti-rabbit and the tertiary antibody was Streptavidin-Cy3 conjugated. Between antibody incubations, slides were washed for 15 min in PBT with at least three changes. The anti-Pbx1 and anti-Pbx123 antibodies were from Santa Cruz Biotechnology Inc. (references P-20 and C-20, respectively), and the anti-Pbx1a

and anti-Pbx1b antibodies were provided by G.H. Swift.

Skeletal preparations

Embryos were eviscerated and the skin removed. After overnight fixation in 95% ethanol, embryos were stained overnight in Alcian blue solution (150 mg Alcian blue (SIGMA), 800 ml 98% ethanol, 200ml acetic acid). After several further hours in 95% ethanol, embryos were transferred to 2% KOH for 24 h. After overnight staining in Alizarin red solution (50mg/l Alizarin red (SIGMA) in 2% KOH), skeletons were cleared in 1% KOH/20% glycerol and stored in 50% ethanol/50% glycerol solution.

Acknowledgements

We are grateful to R. Maxson for the *Msx2* promoter constructs and N. Copeland for the *Meis1a* full-length cDNA. Anti-Pbx1a and anti-Pbx1b were kindly provided by G.H. Swift. We are grateful to Terence Capellini for providing material and helpful discussions. We thank Simon Bartlett for text editing and Alberto Roselló for critical reading of the manuscript. We thank members of the animal house Santiago Rodriguez, José María Fernández and David Esteban for maintaining the *Msx2:Meis1* line. This work was supported by a grant from the Spanish Ministry of Science and Education (BFU2006-10978/BMC). N.M. was supported by Marie Curie fellowship 83EU-056147 and currently by RYC-2006-001694 contract. The CNIC is supported by the Spanish Ministry of Health and Consumer Affairs and the Pro-CNIC Foundation.

References

- ABU-SHAAR, M., RYOO, H.D. and MANN, R.S. (1999). Control of the nuclear localization of extradenticle by competing nuclear import and export signals. *Genes Dev* 13: 935-45.
- AZCOITIA, V., ARACIL, M., MARTINEZ, A.C. and TORRES, M. (2005). The homeodomain protein *Meis1* is essential for definitive hematopoiesis and vascular patterning in the mouse embryo. *Dev Biol* 280: 307-20.
- BERTHELSEN, J., KILSTRUP-NIELSEN, C., BLASI, F., MAVILIO, F. and ZAPPAVIGNA, V. (1999). The subcellular localization of PBX1 and EXD proteins depends on nuclear import and export signals and is modulated by association with PREP1 and HTH. *Genes Dev* 13: 946-53.
- BOULET, A.M. and CAPECCHI, M.R. (2004). Multiple roles of *Hoxa11* and *Hoxd11* in the formation of the mammalian forelimb zeugopod. *Development* 131: 299-309.
- BÜRGLIN, T.R. (1997). Analysis of TALE superclass homeobox genes (MEIS, PBC, KNOX, Iroquois, TGIF) reveals a novel domain conserved between plants and animals. *Nucleic Acids Res* 25: 4173-80.
- CAPDEVILA, J. and IZPISUA BELMONTE, J.C. (2001). Patterning mechanisms controlling vertebrate limb development. *Annu Rev Cell Dev Biol* 17: 87-132.
- CAPDEVILA, J., TSUKUI, T., RODRIQUEZ ESTEBAN, C., ZAPPAVIGNA, V. and IZPISUA BELMONTE, J.C. (1999). Control of vertebrate limb outgrowth by the proximal factor *Meis2* and distal antagonism of BMPs by Gremlin. *Mol Cell* 4: 839-49.
- CAPELLINI, T.D., DI GIACOMO, G., SALS, V., BRENDOLAN, A., FERRETTI, E., SRIVASTAVA, D., ZAPPAVIGNA, V. and SELLERI, L. (2006). Pbx1/Pbx2 requirement for distal limb patterning is mediated by the hierarchical control of Hox gene spatial distribution and Shh expression. *Development* 133: 2263-73.
- CECCONI, F., PROETZEL, G., ALVAREZ-BOLADO, G., JAY, D. and GRUSS, P. (1997). Expression of *Meis2*, a Knotted-related murine homeobox gene, indicates a role in the differentiation of the forebrain and the somitic mesoderm. *Dev Dyn* 210: 184-90.
- CHOE, S.K., VLACHAKIS, N. and SAGERSTROM, C.G. (2002). *Meis* family proteins are required for hindbrain development in the zebrafish. *Development* 129: 585-95.
- DAVIS, A.P. and CAPECCHI, M.R. (1996). A mutational analysis of the 5' *HoxD* genes: dissection of genetic interactions during limb development in the mouse. *Development* 122: 1175-85.
- DAVIS, A.P., WITTE, D.P., HSIEH-LI, H.M., POTTER, S.S. and CAPECCHI, M.R. (1995). Absence of radius and ulna in mice lacking *hoxa-11* and *hoxd-11*. *Nature*

- 375: 791-5.
- DI GIACOMO, G., KOSS, M., CAPELLINI, T.D., BRENDOLAN, A., POPPERL, H. and SELLERI, L. (2006). Spatio-temporal expression of Pbx3 during mouse organogenesis. *Gene Expr Patterns* 6: 747-57.
- DOLLÉ, P., IZPISÚA-BELMONTE, J.C., FALKENSTEIN, H., RENUCCI, A. and DUBOULE, D. (1989). Coordinate expression of the murine Hox-5 complex homeobox-containing genes during limb pattern formation. *Nature* 342: 767-72.
- FRONTAL-RAMAIN, C., WAROT, X., MESSADECQ, N., LEMEURE, M., DOLLE, P. and CHAMBON, P. (1996). Hoxa-13 and Hoxd-13 play a crucial role in the patterning of the limb autopod. *Development* 122: 2997-3011.
- GOFF, D.J. and TABIN, C.J. (1997). Analysis of Hoxd-13 and Hoxd-11 misexpression in chick limb buds reveals that Hox genes affect both bone condensation and growth. *Development* 124: 627-36.
- GONZÁLEZ-CRESPO, S., ABU-SHAAR, M., TORRES, M., MARTÍNEZ-A, C., MANN, R.S. and MORATA, G. (1998). Antagonism between extradenticle function and Hedgehog signalling in the developing limb. *Nature* 394: 196-200.
- HISA, T., SPENCE, S.E., RACHEL, R.A., FUJITA, M., NAKAMURA, T., WARD, J.M., DEVOR-HENNEMAN, D.E., SAIKI, Y., KUTSUNA, H., TESSAROLLO, L. et al. (2004). Hematopoietic, angiogenic and eye defects in Meis1 mutant animals. *EMBO J* 23: 450-9.
- HUANG, H., RASTEGAR, M., BODNER, C., GOH, S.L., RAMBALDI, I. and FEATHERSTONE, M. (2005). MEIS C termini harbor transcriptional activation domains that respond to cell signaling. *J Biol Chem* 280: 10119-27.
- JACOBS, Y., SCHNABEL C.A. and CLEARY M.L. (1999). Trimeric association of Hox and TALE homeodomain proteins mediates Hoxb2 hindbrain enhancer activity. *Mol Cell Biol* 19:5134-42.
- KAMPS, M.P., MURRE, C., SUN, X. and BALTIMORE, D. (1990). A new homeobox gene contributes the DNA binding domain of the t(1;19) translocation protein in pre-B ALL. *Cell* 60: 547-555.
- KILSTRUP-NIELSEN, C., ALESSIO, M. and ZAPPAVIGNA, V. (2003). PBX1 nuclear export is regulated independently of PBX-MEINOX interaction by PKA phosphorylation of the PBC-B domain. *EMBO J* 22: 89-99.
- KMITA, M., TARCHINI, B., ZAKANY, J., LOGAN, M., TABIN, C.J. and DUBOULE, D. (2005). Early developmental arrest of mammalian limbs lacking HoxA/HoxD gene function. *Nature* 435: 1113-6.
- KNEZEVIC, V., DE SANTO, R., SCHUGHART, K., HUFFSTADT, U., CHIANG, C., MAHON, K.A. and MACKEM, S. (1997). Hoxd-12 differentially affects preaxial and postaxial chondrogenic branches in the limb and regulates Sonic hedgehog in a positive feedback loop. *Development* 124: 4523-36.
- LEHOCZKY, J.A., WILLIAMS, M.E. and INNIS, J.W. (2004). Conserved expression domains for genes upstream and within the HoxA and HoxD clusters suggests a long-range enhancer existed before cluster duplication. *Evol Dev* 6: 423-30.
- LIU, Y.H., MA, L., WU, L.Y., LUO, W., KUNDU, R., SANGIORGI, F., SNEAD, M.L. and MAXSON, R. (1994). Regulation of the Msx2 homeobox gene during mouse embryogenesis: a transgene with 439 bp of 5' flanking sequence is expressed exclusively in the apical ectodermal ridge of the developing limb. *Mech Dev* 48: 187-97.
- MAEDA, R., ISHIMURA, A., MOOD, K., PARK, E.K., BUCHBERG, A.M. and DAAR, I.O. (2002). Xpbx1b and Xmeis1b play a collaborative role in hindbrain and neural crest gene expression in *Xenopus* embryos. *Proc Natl Acad Sci USA* 99: 5448-53.
- MANN, R.S. and AFFOLTER, M. (1998). Hox proteins meet more partners. *Curr Opin Genet Dev* 8: 423-9.
- MERCADER, N., LEONARDO, E., AZPIAZU, N., SERRANO, A., MORATA, G., MARTINEZ, C. and TORRES, M. (1999). Conserved regulation of proximodistal limb axis development by Meis1/Hth. *Nature* 402: 425-9.
- MERCADER, N., LEONARDO, E., PIEDRA, M.E., MARTINEZ, A.C., ROS, M.A. and TORRES, M. (2000). Opposing RA and FGF signals control proximodistal vertebrate limb development through regulation of Meis genes. *Development* 127: 3961-70.
- MERCADER, N., TANAKA, E.M. and TORRES, M. (2005). Proximodistal identity during vertebrate limb regeneration is regulated by Meis homeodomain proteins. *Development* 132: 4131-42.
- MONICA, K., GALILI, N., NOURSE, J., SALTMAN, D. and CLEARY, M.L. (1991). PBX2 and PBX3, new homeobox genes with extensive homology to the human proto-oncogene PBX1. *Mol Cell Biol* 11: 6149-57.
- MORGAN, B.A., IZPISÚA-BELMONTE, J.C., DUBOULE, D. and TABIN, C.J. (1992). Targeted misexpression of Hox-4.6 in the avian limb bud causes apparent homeotic transformations. *Nature* 358: 236-9.
- MOSKOW, J.J., BULLRICH, F., HUEBNER, K., DAAR, I.O. and BUCHBERG, A.M. (1995). Meis1, a PBX1-related homeobox gene involved in myeloid leukemia in BXH-2 mice. *Mol Cell Biol* 15: 5434-43.
- NAKAMURA, T., JENKINS, N.A. and COPELAND, N.G. (1996). Identification of a new family of Pbx-related homeobox genes. *Oncogene* 13: 2235-42.
- NELSON, C.E., MORGAN, B.A., BURKE, A.C., LAUFER, E., DIMAMBRO, E., MURTAUGH, L.C., GONZALES, E., TESSAROLLO, L., PARADA, L.F. and TABIN, C. (1996). Analysis of Hox gene expression in the chick limb bud. *Development* 122: 1449-66.
- NOURSE, J., MELLENTIN, J.D., GALILI, N., WILKINSON, J., STANBRIDGE, E., SMITH, S.D. and CLEARY, M.L. (1990). Chromosomal translocation t(1;19) results in synthesis of a homeobox fusion mRNA that codes for a potential chimeric transcription factor. *Cell* 60: 535-545.
- OULAD-ABDELGHANI, M., CHAZAUD, C., BOUILLET, P., SAPIN, V., CHAMBON, P. and DOLLÉ, P. (1997). Meis2, a novel mouse Pbx-related homeobox gene induced by retinoic acid during differentiation of P19 embryonal carcinoma cells. *Dev Dyn* 210: 173-83.
- POPPERL, H., RIKHOF, H., CHANG, H., HAFFTER, P., KIMMEL, C.B. and MOENS, C.B. (2000). Iazarus is a novel pbx gene that globally mediates hox gene function in zebrafish. *Mol Cell* 6: 255-67.
- POST, L.C. and INNIS, J.W. (1999). Altered Hox expression and increased cell death distinguish Hypodactyly from Hoxa13 null mice. *Int J Dev Biol* 43: 287-94.
- PRPIC, N.M., JANSSEN, R., WIGAND, B., KLINGLER, M. and DAMEN, W.G. (2003). Gene expression in spider appendages reveals reversal of exd/hth spatial specificity, altered leg gap gene dynamics, and suggests divergent distal morphogen signaling. *Dev Biol* 264: 119-40.
- RIBES, V., OTTO, D.M., DICKMANN, L., SCHMIDT, K., SCHUHBAUR, B., HENDERSON, C., BLOMHOFF, R., WOLF, C.R., TICKLE, C. and DOLLE, P. (2007). Rescue of cytochrome P450 oxidoreductase (Por) mouse mutants reveals functions in vasculogenesis, brain and limb patterning linked to retinoic acid homeostasis. *Dev Biol* 303: 66-81.
- RIECKHOF, G.E., CASARES, F., RYOO, H.D., ABU-SHAAR, M. and MANN, R.S. (1997). Nuclear translocation of extradenticle requires homothorax, which encodes an extradenticle-related homeodomain protein. *Cell* 91: 171-83.
- SATO, K., KOIZUMI, Y., TAKAHASHI, M., KUROIWA, A. and TAMURA, K. (2007). Specification of cell fate along the proximal-distal axis in the developing chick limb bud. *Development* 134: 1397-406.
- SAUNDERS, J.W. (1948). The proximodistal sequence of origin of the parts of the chick wing and the role of the ectoderm. *J. Exp. Zool.* 108: 363-403.
- SELLERI, L., DEPEW, M.J., JACOBS, Y., CHANDA, S.K., TSANG, K.Y., CHEAH, K.S., RUBENSTEIN, J.L., O'GORMAN, S. and CLEARY, M.L. (2001). Requirement for Pbx1 in skeletal patterning and programming chondrocyte proliferation and differentiation. *Development* 128: 3543-57.
- SPITZ, F., GONZALEZ, F. and DUBOULE, D. (2003). A global control region defines a chromosomal regulatory landscape containing the HoxD cluster. *Cell* 113: 405-17.
- STADLER, H.S., HIGGINS, K.M. and CAPECCHI, M.R. (2001). Loss of Eph-receptor expression correlates with loss of cell adhesion and chondrogenic capacity in Hoxa13 mutant limbs. *Development* 128: 4177-88.
- SUCOV, H.M., IZPISUA-BELMONTE, J.C., GANAN, Y. and EVANS, R.M. (1995). Mouse embryos lacking RXR alpha are resistant to retinoic-acid-induced limb defects. *Development* 121: 3997-4003.
- SUMMERBELL, D., LEWIS, J. and WOLPERT, L. (1973). Positional information in chick limb morphogenesis. *Nature* 224: 492-496.
- SUZUKI, M. and KUROIWA, A. (2002). Transition of Hox expression during limb cartilage development. *Mech Dev* 118: 241-5.
- TABIN, C. and WOLPERT, L. (2007). Rethinking the proximodistal axis of the vertebrate limb in the molecular era. *Genes Dev* 21: 1433-42.
- TICKLE, C. (2002). Molecular basis of vertebrate limb patterning. *Am J Med Genet* 112: 250-5.
- VLACHAKIS, N., CHOE, S.K. and SAGERSTROM, C.G. (2001). Meis3 synergizes

- with Pbx4 and Hoxb1b in promoting hindbrain fates in the zebrafish. *Development* 128: 1299-312.
- WILKINSON, D.G. and NIETO, M.A. (1993). Detection of messenger RNA by *in situ* hybridization to tissue sections and whole mount. *Methods Enzymol.* 225: 361-373.
- YASHIRO, K., ZHAO, X., UEHARA, M., YAMASHITA, K., NISHIJIMA, M., NISHINO, J., SAJJOH, Y., SAKAI, Y. and HAMADA, H. (2004). Regulation of retinoic acid distribution is required for proximodistal patterning and outgrowth of the developing mouse limb. *Dev Cell* 6: 411-22.
- YOKOUCHI, Y., NAKAZATO, S., YAMAMOTO, M., GOTO, Y., KAMEDA, T., IBA, H. and KUROIWA, A. (1995). Misexpression of Hoxa-13 induces cartilage homeotic transformation and changes cell adhesiveness in chick limb buds. *Genes Dev* 9: 2509-22.
- YOKOUCHI, Y., SASAKI, H. and KUROIWA, A. (1991). Homeobox gene expression correlated with the bifurcation process of limb cartilage development. *Nature* 353: 443-5.
- ZAKANY, J. and DUBOULE, D. (1999). Hox genes in digit development and evolution. *Cell Tissue Res* 296: 19-25.

Related, previously published *Int. J. Dev. Biol.* articles

See our recent Special Issue **Ear Development** edited by Bernd Fritzsch and Fernando Giraldez at: <http://www.ijdb.ehu.es/web/contents.php?vol=51&issue=6-7>

See our Special Issue **Limb Development** edited by Juan Hurlé and Juan Carlos Izpisua-Belmonte at: <http://www.ijdb.ehu.es/web/contents.php?vol=46&issue=7>

PBX proteins: much more than Hox cofactors

Audrey Laurent, Réjane Bihan, Francis Omilli, Stéphane Deschamps and Isabelle Pellerin
Int. J. Dev. Biol. (2008) 52: 9-20

A comparative analysis of Meox1 and Meox2 in the developing somites and limbs of the chick embryo

Susan Reijntjes, Sigmar Stricker and Baljinder S. Mankoo
Int. J. Dev. Biol. (2007) 51: 753-759

Analysis of a new allele of limb deformity (ld) reveals tissue- and age-specific transcriptional effects of the Ld Global Control Region

Emilia Pavel, Wenning Zhao, Kimerly A. Powell, Michael Weinstein and Lawrence S. Kirschner
Int. J. Dev. Biol. (2007) 51: 273-281

The expression of Fat-1 cadherin during chick limb development

Terence G. Smith, Nick Van Hateren, Cheryll Tickle and Stuart A. Wilson
Int. J. Dev. Biol. (2007) 51: 173-176

The expression of Flrt3 during chick limb development

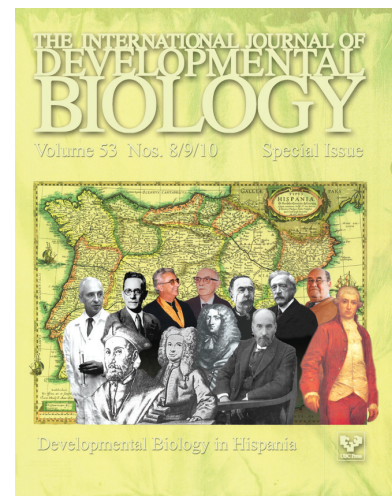
Terence G. Smith and Cheryll Tickle
Int. J. Dev. Biol. (2006) 50: 701-704

PBX1 intracellular localization is independent of MEIS1 in epithelial cells of the developing female genital tract

Agnès Dintilhac, Réjane Bihan, Daniel Guerrier, Stéphane Deschamps, Héloïse Bougerie, Tanguy Watrin, Georgette Bonnac and Isabelle Pellerin
Int. J. Dev. Biol. (2005) 49: 851-858

Pbx genes are required in *Xenopus* lens development

Richard Morgan, Jastinder Sohal, Mita Paleja and Ruth Pettengell
Int. J. Dev. Biol. (2004) 48: 623-627



5 yr ISI Impact Factor (2008) = 3.271

